RAINFALL VARIABILITY AT THE END OF THE DRY SEASON OVER THE SOUTHERN AMAZON BASIN

Guillermo O. Obregón* and Carlos A. Nobre

Center for Weather Forecasting and Climate Studies – CPTEC-INPE

1. INTRODUCTION

The last few years witnessed a lively discussion about the meteorological impact of the smoke from Amazonian forest fires along the smoke plumes. It seems that biomass burning aerosol impacts on cloud formation and microphysical processes may be of importance mostly at the end of the dry season and beginning of the wet season.

The deforestation in the Amazon basin has been increased in the last decades. The forest fires emit large amounts of cloud condensation nuclei (CCN) into the atmosphere which makes CCN concentration be an order of magnitude higher than the natural background concentration possible affecting the cloud the cloud microphysics (Andreae et al., 2002). The higher concentration of CCD reduce cloud drop size and may delay the onset of rainfall at different highs above cloud base, related to the cloud type, and further the elevation of CCN to the upper troposphere can cause intense thunderstorms (Andreae et al., 2004). Koren, et al. (2004) shows observational evidence of reduction from 38% (clean conditions) to 0% (heavily smoke) of scattered cumulus cloud over Amazon during the biomass burning. Feingold et al. (2005) using large eddy simulations of smoke-cloud interactions to study the cloud suppression in biomass burning regions of Amazonia, concluded that the vertical distribution of the smoke aerosol in the convective boundary layer is decisive, since aerosol resident in the boundary layer where the cloud tends to form reduces cloudiness and the aerosol emitted in a daytime convective boundary layer may reduce or increase cloudiness. On the other hand, rainfall analysis shown that the El Niño Southern Oscillation (ENSO) phenomenon has a weak influence at seasonal time scales on the rainfall over the area of study (e.g. Aceituno, 1988).

The aim of this study is to analyze daily and monthly historical rainfall time series longer than 30 years of records for August-September for raingauges located along the smoke plume over Southern Amazonia in search of trends that could be attributed to biomass burning effects, because during the earlier part of the record, biomass burning was not extensive as opposed to the later part of the record.

2. MATERIALS AND METHODS

The main data in this study is the daily rainfall time series for August-September from four raingauges distributed around southern Amazon basin (Fig. 1).
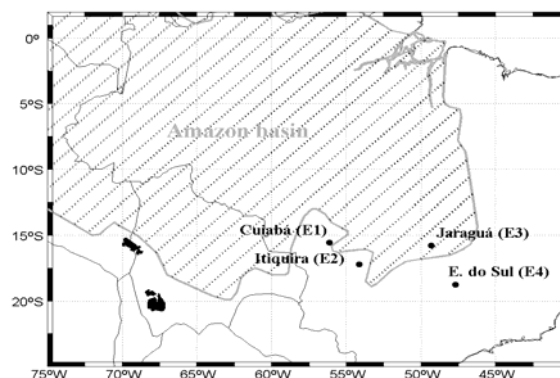
Figure 1 - Study area. Raingauges around southern Amazon basin.

The rainfall gauges location and the period of the record are shown in the Table I. For convenience the name of the raingauges location will be named as E1, E2, E3 and E4. A full quality control was carried out for all daily rainfall data.

TABLE 1 – Raingauges Characteristics

	Lat.	Lon.	Start	End
Cuiabá	15.55°S	56.11°W	1961	2000
Itiquirá	17.20°S	54.13°W	1966	2003
Jaraguá	15.75°S	49.32°W	1964	2003
E. do Sul	18.73°S	47.69°W	1944	2003

. In order to find inter-annual components of the monthly total rainfall time series, the empirical mode decomposition (EMD) method developed by Huang et al. (1998) was applied to the total monthly rainfall for August and September, to determine different time scales of the monthly rainfall variability and their related marginal spectrum are calculated. The EMD method can decompose a time series into finite components, called intrinsic mode functions (IMF), and a trend. Each IMF component contains different time scale that would help to find possible mechanisms related to large scale global circulation or to the impact of the smoke from Amazon fires on rainfall. Additional analysis of the inconditional probability of wet days, the frequency of rainfall

intensities from small to intense ones and the variability of the daily rainfall appear to be the most suitable way to search a probable trend along the rainfall record as indicative of the effect of the Amazon fires on rainfall. Linear correlation between the standardized monthly rainfall and the IMF modes with the indices of the ENSO (SOI), Pacific Decadal Oscillation (PDO) and the Antarctic Oscillation (AOO) are also considered in this study.

3. RESULTS AND DISCUSSION

3.1 Monthly rainfall variability and their teleconnectoins

Fig. 2a-b shows the temporal variation of the total monthly rainfall of August and September for the four rainfall stations. The EMD slower components, residual (trend), are also included in all monthly rainfall series. Besides the noisy inter-annual rainfall distribution in August in the four rainfall stations, Fig. 2a shows a coherent characteristic, the maximal rainfall occurs at around the last part of the 1980's. The trend is positive in three places, except at E2, where it shows a parabolic shape. The trend at E1 and at E4 apparently suffers a shift in intensify at the middle of the 1970's, and it probably is related to the large scale quasi-decal oscillation "like ENOS" (Zhang, et al., 1997). It appears controversial that only two among four rainfall stations shown that fact, but as it is well-known that the length of the time series is critical for any trend analysis, and the short length of the time series of E2 and E3 can be explained by this feature. Also, the Mann-Kendall test shows that only in E4 the linear trend is significant at the level of 95%.

The inter-annual rainfall variability in September is characterized by periods apparently quasi-cyclic along all the record and rainfall stations (Fig. 2b). At E4 the inter-annual variability shows quasi-cyclic periods shorter than in the other rainfall stations. At the E1 and the E2 is observed coherent maximum peaks of rainfall around 1970 and 1980. Positive rainfall trend are observed in rainfall stations, with exception of the E3, where the trend seems to indicate a rainfall decrease. Also, as it was in August, the trend appears to show a positive shift in the middle of the 1970's and in the same rainfall stations, E1 and E4, and also the E4 shows a significant linear trend at the level of 95% in this month.

In order to find some relationships between the rainfall and the different global phenomenon, the correlation between the standardized monthly rainfall and the different indices of global scale phenomenon was calculated. The results show that the correlation coefficient (c.c.) between three indices and the rainfall is significant at levels more than 90%., and

apparently there are different driver for rainfall at different stations and months. In August, the ENOS and the rainfall show negative correlation and it appears restrict to the E1 (c.c. = -.27) and E2 (c.c. = -.42), whereas rainfall and the PDO (c.c. =.38) and AOO (c.c. = 23) have direct relationship with E4 in September.
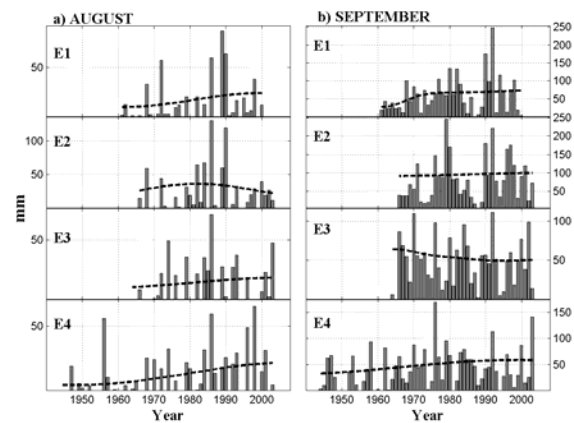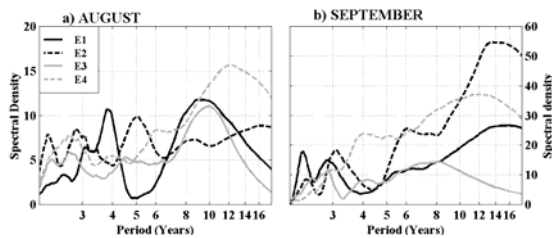

Figure 2 - Total monthly rainfall (mm) for August (left) and September (right). From top to bottom are the rainfall gauges as indicated in Table I. The hatched line is the residual (trend) of the EMD components.

3.2 EMD analysis of monthly rainfall

The EMD of the monthly times series for August and September (not shown) can be better analyzed by their related marginal spectrum. Fig. 3a-b shows the marginal spectrum for the monthly rainfall of August and September for all the rainfall stations. They are constructed by the recombination of all the modes of the EMD. Each month and rainfall station presents a typical feature with different peaks in periods from inter-annual variability (2-5 years) up to inter decadal scales (8-14 years), which reveals the strong complexity of the rainfall variability over this region. It is necessary to point out that there is no method to calculate the significance of this spectrum, but the relative difference at inter-annual and the quasi inter-decadal values between August and September to be able to assit in the analysis.

At inter-annual scales (2-3 years) rainfall stations E2, E3 and E4 show distinctive peaks in August, and rainfall stations E1, E2 and E3 in September. Also, strong peaks around 4 years and 5 years are shown in August in E1 and E2, respectively, and in September the E4 shows an apparently weak peak at around 4 years. The results observed at inter-annual periods are consistent with the two distinct ENSO periods, designate as high (2-3 year period) and low (3-8 year period) frequency (Barnett, 1991), and it seems that the teleconnection between

the rainfall and the ENOS is strongest in August than in September, mainly in E1 and E2, because their peaks are clearly perceived in this month and it is corroborated by the significant correlation coefficient discussed above. At quasi-decadal scales (8-14 years) a peak around the period of 9-10 years is shown for E1 and E3, and a peak at period of 12 years is observed in E4 in August, and apparently during this month at this scale there is a relationship with large scale circulation phenomenon, as it is shown by the correlation coefficients. In the same scale, the rainfall spectrum of September shows a peak between 12-16 years in E1 and E2, and a peak with period around 12 years in E4.

Figure 3 - Marginal Spectrum of the recombination of all modes of the monthly rainfall for August (left) and September (right).

The result obtained seems to indicate that the teleconnections between ENOS and the rainfall is restricted to August and at rainfall stations located at western portion of the area of study, and at inter-annual scales the teleconnections appears more evident in September related to PDO and AOO and restricted to the southern part. In both months August and September the large scale phenomenon strengthening the rainfall occurrence.

To demonstrate the relation of rainfall modes with large scale phenomenon is carry out a correlation between the index of each phenomenon with all modes of each monthly rainfall is calculated, except the lower mode (trend) showed in Fig. 2. The results, displayed in Fig. 3, shown that the ENSO are related to inter-annual variability of rainfall mainly in August, where the second mode of E1 (E1M2), the E2M2 shown coherent oscillation of around of 4-5 year from 1970 and the E4M3 has oscillation whit larger periods. Also, the other Quasi-decadal oscillations AOO and PDO are related to E3M1 and E3M4, respectively, in August. Similarly, in September oscillations quasi-decadal and larger are the main driver of rainfall in E2, E3 and E4. The rainfall modes E3M2 and E4M3 with quasi-decadal periods are related to AOO, likewise period larger than quasi-decadal E2M4 and E3M3 are related to the PDO. Hence, the EMD of monthly rainfall has been improved the knowledge of the teleconecctions between the rainfall at the area of study and the large scale circulation.
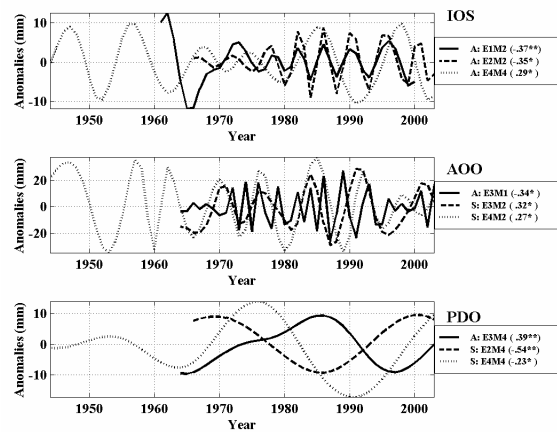

Figure 3 - The intrinsic modes (M) of monthly Rainfall of August (A) and September (S) for the different rainfall stations (E1, E2, E3 and E4), related to IOS, AOO and PDO. It was obtained by means of their significant correlation coefficient between each mode with every index. The c.c. and its significance are indicates in the legend.

3.3 Conditional Probability of daily rainfall

The daily rainfall data are used to calculate the incondicional probability of wet days and to detect the frequency distribution of rain intensities along all the record. The distribution of the wet days for each month (more than 1 mm) and the frequency of the daily rainfall intensities, divided in light (1- 5 mm), moderated (5- 25 mm) and intense (> 25 mm) can be seen as an index of the inter-annual rainfall variability, and that would help find more precisely the impact of the smoke from Amazon fires on rainfall. In these sense the distribution of wet days and the frequency of rainfall intensities for periods of five years was calculated.

Fig. 4 shows the variability of the incondicional probability of wet days in percent for periods of five years for each four rainfall station and month. From Fig. 4a we can see that for August the wettest five years occurred between 1986 and 1990 in all the rainfall stations. The values for this period are from two to three times greater than the rest of the periods, which are less than 5 % (1-2) of rainfall days per month. Apparently there is no linear trend, but a jump and return to values around normally. In September (Fig. 4b) the wettest period is observed between 1976 and 1980, and it is less notable than the wettest period observed in August. A noteworthy feature in September is the apparent increased of wet days along the period, reached its maxima in 1976-1980, then decreases and becomes stable in the last years of the record.

The frequency distribution of the daily intensities from August and September for 5-years periods is shown in Fig. 5a-b. Actually, it is hard to find a specific pattern for intense rainfall for all the rainfall stations in the two months. In August (Fig. 5a) there is a decrease of days with light rainfall, apparently compensated by days with moderated rainfall, and the wettest period of 1986-1990 is mainly due to moderated rainfall with some contribution of intense rainfall.
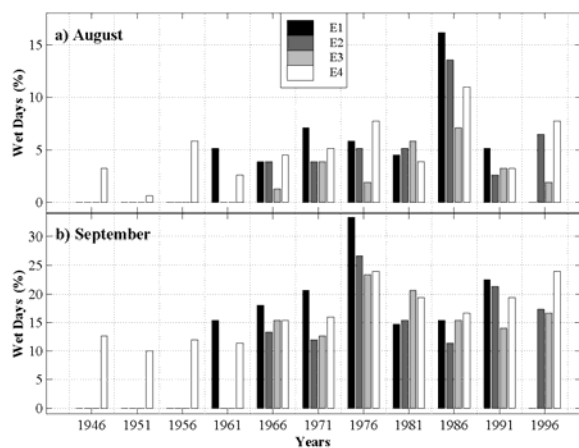
Figure 4 - Incondicional probabilities of wet days (%) for periods of 5 years.   August (a) and September (b).

Fig. 5b shows the frequency distribution for September. Comparison of the distribution of E2 in September with August suggests that there is a similar decrease of days with light rainfall, and increased of days with moderated rainfall and some with intense rainfall, which do not occur in the other rainfall stations. There is a hint of increase of days with intense rainfall in station of E1.   The patterns of frequencies observed in both the conditional probability of wet day and the frequency of intensities show that there is no clear evidence of decrease of rainfall along the record.   The frequency of wet day is certainly modulated by the large scale circulation even if it is not observed in Fig. 4, because it was smoothed for the five years periods. Additionally the frequency distribution of rainfall intensities are noisy in the almost all of the stations.
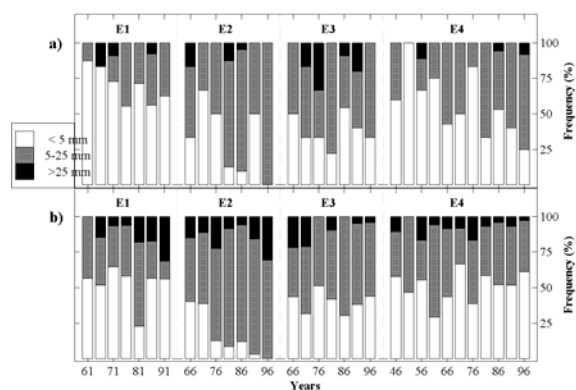
Figure 5: Frequency of the daily rainfall intensities (%) for periods of 5 years. Light rainfall (< 5 mm) moderated (5-25 mm) and intense (> 25 mm).

4. CONCLUSIONS

In this study, a 38 –years record of daily rainfall of four raingauges south of Amazonia are used to find the probable meteorological impact of the smoke aerosol from Amazonian forest fires along the smoke plumes

on the rainfall at the end of the dry season.   The EMD method is applied to decompose the monthly rainfall time series into different IMF components and the marginal spectrum was calculated in addition to the daily frequency of incondicional probabilities of wet days and frequency intensities.   Indices of large scale circulation are also used to search for possible planetary-scale relationship that could be underlying mechanisms driving rainfall variability.

Some major findings are summarized as follows:

1) - The ENSO influence in the rainfall at inter-annual scales, mainly in August, appears to be associated to increasing amounts of rainfall, and it appears more intense at the western part of the study area. Meanwhile, it is found that Pacific Decadal Oscillation and the Antarctic Oscillations are the large scale circulations features related to rainfall in September.

2) The slowest varying mode (residue) seems to represent the rainfall long term trend. With exception of Itiquirá (E2) in August and Jaraguá (E3) in September, the rainfall trend for all the rainfall stations and in both months August and September is positive. Notwithstanding the small number of stations utilized in the analysis, the results indicate that, if biomass burning smoke effects are present in Southern Amazonia at the end of the dry season inhibiting rainfall, those effects may be masked by large scale controls over rainfall producing mechanisms. That would call for detailed experimental plans to single out the possible effect of smoke on rainfall over Amazonia..

REFERENCES

Aceituno, P., 1988: On the functioning of the Southern Oscillation in South America sector- Part I: *Surface Climate. Mon Weather Rev.,* **116**, 505-524.

Andreae, M. O., et al., 2002: Biogeochemical cycling of carbon, water, energy, trace gases and aerosols in Amazonia: The LBA_EUSTACH experiments. *J. Geophys. Res.,* **107,** 10.1029/2001JD000666.

Andreae, M. O., D. Rosenfeld, P. Artaxo, A. A. costa, G. P. Frank, K. M. Longo, M. A. F. Silva-Dias, 2004*: Smoking Rain Clouds over the Amazon. Science,* **303,** 1337-1342.

Barnett, T. P., 1991: The interaction of multiple time scales in the Tropical climate system. **J. Climate, 4,** 169-185

Feingold G., Hongli Jiang, Jerry Y. Harrington, 2005: On Smoke Suppression of Clouds in Amazonia. *Geophys. Res. Lett., 32***,** 10.1029/2004GL021369.

Koren, Ila, Yora, J. Kaufman, Lorraine A. Remer, Jose V. Martins, 2004: *Measurements of the Effect of Amazon Smoke on Inhibition of Cloud Formation. Science,* **303,** 1342-1345

Huang, N. E., Z. Shen, S. R. Long, M. C. Wu, and H. H. Shih, 1998: The empirical mode decomposition and Hilbert spectrum for nonlinear and non-stationary time series analysis. *Proc. R. Soc. London Ser.,* **A454,**   903-995.

Zhang, Y, Wallace J. M., Battitsi, D. E., 1997: ENSO-like interdecadal variability: 1900-93. *J Climate,* **10,** 1004-1020.